ORIGINAL ARTICLE

Xenotransplantation WILEY

Genetic knockout of porcine *GGTA1* or *CMAH/GGTA1* is associated with the emergence of neo-glycans

Lucrezia Morticelli[1] | Charlotte Rossdam[2] | Samanta Cajic[3,4] | Dietmar Böthig[5] |
Mikhail Magdei[1] | Sugat Ratna Tuladhar[5] | Björn Petersen[6] | Konrad Fischer[7] |
Erdmann Rapp[3,4] | Sotirios Korossis[8] | Axel Haverich[1,5] | Angelika Schnieke[7] |
Heiner Niemann[9] | Falk F. R. Buettner[2] | Andres Hilfiker[1,5]

[1]Leibniz Research Laboratories for Biotechnology and Artificial Organs (LEBAO), Hannover Medical School, Hannover, Germany

[2]Institute of Clinical Biochemistry, Hannover Medical School, Hannover, Germany

[3]Max Planck Institute for Dynamics of Complex Technical Systems, Magdeburg, Germany

[4]glyXera GmbH, Magdeburg, Germany

[5]Department of Cardiothoracic, Transplantation and Vascular Surgery, Hannover Medical School, Hannover, Germany

[6]Institute of Farm Animal Genetics, Friedrich-Loeffler-Institut, Mariensee/Neustadt am Ruebenberge, Germany

[7]Chair of Livestock Biotechnology, School of Life Sciences Weihenstephan, Technische Universität München, Freising, Germany

[8]Cardiopulmonary Regenerative Engineering (CARE) Group, Centre for Biological Engineering (CBE), Wolfson School of Mechanical, Electrical and Manufacturing Engineering, Loughborough University, Loughborough, UK

[9]Clinic for Gastroenterology, Hepatology & Endocrinology, Hannover Medical School (MHH), Hannover, Germany

Correspondence
Falk F. R. Buettner, Hannover Medical School, Carl-Neuberg-Strasse 1, 30625 Hannover, Germany.
Email: buettner.falk@mh-hannover.de

Abstract

Background: Pig-derived tissues could overcome the shortage of human donor organs in transplantation. However, the glycans with terminal α-Gal and Neu5Gc, which are synthesized by enzymes, encoded by the genes *GGTA1* and *CMAH*, are known to play a major role in immunogenicity of porcine tissue, ultimately leading to xenograft rejection.

Methods: The *N*-glycome and glycosphingolipidome of native and decellularized porcine pericardia from wildtype (WT), *GGTA1*-KO and *GGTA1/CMAH*-KO pigs were analyzed by multiplexed capillary gel electrophoresis coupled to laser-induced fluorescence detection.

Results: We identified biantennary and core-fucosylated *N*-glycans terminating with immunogenic α-Gal- and α-Gal-/Neu5Gc-epitopes on pericardium of WT pigs that were absent in *GGTA1* and *GGTA1/CMAH*-KO pigs, respectively. Levels of *N*-glycans terminating with galactose bound in β(1-4)-linkage to *N*-acetylglucosamine and their

---

Lucrezia Morticelli, Charlotte Rossdam, Falk F. R. Buettner, and Andres Hilfiker contributed equally.

- -

derivatives elongated by Neu5Ac were increased in both KO groups. *N*-glycans capped with Neu5Gc were increased in *GGTA1*-KO pigs compared to WT, but were not detected in *GGTA1/CMAH*-KO pigs. Similarly, the ganglioside Neu5Gc-GM3 was found in WT and *GGTA1*-KO but not in *GGTA1/CMAH*-KO pigs. The applied detergent based decellularization efficiently removed GSL glycans.

Conclusion: Genetic deletion of *GGTA1* or *GGTA1/CMAH* removes specific epitopes providing a more human-like glycosylation pattern, but at the same time changes distribution and levels of other porcine glycans that are potentially immunogenic.

1 | INTRODUCTION

Clinical application of xenogeneic tissue holds great potential to overcome human donor organ shortage, in particular in the younger population.[1,2] Several types of porcine, bovine, and equine tissues have been used for applications in cardiac, orthopedic, esophageal, and urinary tract surgery.[2] In particular, porcine or bovine pericardium has been extensively used for the production of heart valves chemically fixed in glutaraldehyde (GA), also known as bioprosthetic heart valves (BHVs).[3–6] Unfortunately, BHVs are associated with structural valve deterioration (SVD), in particular in patients below 60 years of age.[3,6] SVD of BHVs has been correlated to GA fixation and to the presence of glycan xenoantigens.[7–10] Indeed, in addition to protein xenoantigens, carbohydrate antigens seem to play a major role in tissue immunogenicity due to immense variability, both within and between species, and considerably greater than that of proteins.[11] The immune response induced by glycan xenoantigens is mainly humoral, and driven by natural and pre-existing antibodies.[2] The major glycan structures associated with an adverse immune response are the Galα1–3 Gal (α-Gal) epitopes, found as terminal residue on *N*-glycans and glycolipids, and the non-human sialic acid *N*-glycolylneuraminic acid (Neu5Gc), also known as Hanganutziu–Deicher antigen, found in *N*-, *O*-glycans and glycolipids.[12,13] Both xenoantigens are not synthesized in humans due to inactivation of genes encoding the enzymes *N*-acetyllactosaminide alpha-1,3-galactosyltransferase (GGTA1) and cytidine monophosphate-*N*-acetylneuraminic acid hydroxylase (CMAH). Interestingly, humans express circulating IgA/IgG/IgM antibodies against α-Gal and Neu5Gc.[5] The α-Gal epitope on xenogeneic tissue has been associated with hyperacute graft rejection, whereas Neu5Gc is involved in the acute graft rejection process observed upon transplantation of xenogeneic tissue/organs in humans.[14,15] Neu5Gc has been identified in human tissues; as it can be introduced with meat- and milk-derived dietary products. Despite its incorporation in human tissues, Neu5Gc is recognized as non-self by the immune system, which in turn induces high levels of polyclonal anti-Neu5Gc antibodies.[2]

Decellularization of allografts and xenografts has been successfully used to remove cellular material, with the goal to render organs suitable for transplantation, that is, to become immunologically compatible and capable of growing within the patient.[16] Different chemical, enzymatic, and physical techniques have been tested for decellularization to remove the known immunogenic compounds, such as cells and water-soluble molecules.[16] However, for elimination of carbohydrate xenoantigens, blocking their synthesis has proven to be most efficient. Gene-edited pigs lacking the expression of both α-Gal and Neu5Gc were produced for the construction of safer xenografts.[17,18] The use of such xenografts decreased antibody binding to porcine tissue. As an example, in vivo short-term studies using *GGTA1* knockout stented GA fixed BHVs, (lacking the expression of α-Gal), transplanted into non-human primates, showed a lower immune response compared to the standard biological heart valves isolated from wildtype animals.[19] Furthermore, triple transgenic (*GGTA1*-KO/human CD46/human thrombomodulin) pig heart heterotrophically transplanted into baboons with various immunomodulatory strategies prevented graft rejection and resulted in graft survival beyond 900 days.[20] Other studies showed that long-term graft failure still occurs, unless using strong immunomodulatory strategies.[21,22]

While genetic engineering of donor pigs can knockout the expression of known xenoantigens, it could also induce the increased expression of pre-existing sugar residues, or the de novo appearance of glycans.[23,24] Previous studies have shown that deletion of the GGTA1 and CMAH proteins resulted in an increased production of high mannose and truncated glycans, xylosylation and increased fucosylation on *N*-linked glycans isolated from serum proteins of *GGTA1/CMAH*-KO pigs.[23] These types of sugar structures are only present in low amounts in humans and might induce different types of immune responses.

In the current study, we investigated the effects of genetic knockout of two important glycan epitopes on the porcine glycome using porcine pericardium as a model. By using multiplexed capillary gel electrophoresis coupled to laser induced fluorescence detection (xCGE-LIF), we interrogated *N*-glycosylation and glycosphingolipid glycosylation of native and decellularized porcine pericardium of WT, *GGTA1*- and *GGTA1/CMAH*-KO pigs focussing on the potential emergence of neo-glycoepitopes that might act as novel xenogeneic determinants.

2 | MATERIALS AND METHODS

2.1 | Tissue collection and preparation

Heart valves were either obtained from 6-months old German Landrace pigs (wildtype (WT) pigs) from a local slaughterhouse (Merhold GmbH), from *GGTA1*-KO pigs (Friedrich-Loeffler-Institut, Mariensee)[25] or from a *GGTA1/CMAH*-KO pig (School of Life Sciences Weihenstephan, TUM, Freising).[17] The parietal layer of the pericardium was isolated from the heart and the excess fat and tissue were trimmed carefully. Out of six WT porcine heart valves, three pericardia were left untreated (WT native, $n = 3$) and three were processed for decellularization as described below (WT decellularized, $n = 3$). Out of two pericardia obtained from *GGTA1*-KO pigs, half of each was left untreated (*GGTA1*-KO native, $n = 2$) and the other half was decellularized (*GGTA1*-KO decellularized, $n = 2$). Of one pericardium from a *GGTA1/CMAH*-KO pig half was left untreated (*GGTA1/CMAH*-KO native, $n = 1$) and the other half was decellularized (*GGTA1/CMAH*-KO decellularized, $n = 1$). Untreated material was stored at $-20°C$ for further processing for *N*-glycans analysis as described below.

2.2 | Decellularization

The pericardia were decellularized with a modified version of the protocol for decellularization of porcine pulmonary valves, described previously.[26] Briefly, nine pericardia (size 7×10 cm each) were placed individually in 250 mL square Schott bottles and disinfected in 70 mL of an antibiotic cocktail, made of 0.2 mg/mL polymyxin B sulfate (Sigma P4932), 0.05 mg/mL vancomycin hydrochloride hydrate (Sigma-Aldrich 861987), and 0.5 mg/mL gentamicin sulfate (Biochrom A271-25), at 37°C for 1 h. Following disinfection, tissues were first washed in hypotonic buffer (10 mM Tris, 2.7 mM EDTA), subsequently treated with 0.5% (v/v) Triton X-100 and then with 0.5% (w/v) SDS, each step for 24 h at RT. Following treatment in detergents, samples were washed 12 times with PBS (12 h for each wash) at RT. Each step of the protocol was carried out under agitation (180 rpm) in an elliptical shaker (GFL 3031), using 140 mL liquid, unless otherwise stated. Samples were stored in 50 mL reaction tubes in PBS with 1% v/v penicillin/streptomycin at 4°C until analysis.

2.3 | N-glycan analysis

N-glycans were analyzed by multiplexed capillary gel electrophoresis coupled to laser-induced fluorescence (xCGE-LIF) as described previously,[27] with some modifications. Tissue samples of native and decellularized pericardia were cryogenically grinded with a mortar and pestle upon freezing in liquid nitrogen. Then, samples were freeze-dried and 5 mg (dry weight) of each sample was further incubated with collagenase type 2 (Worthington Biochemical Corporation, USA)

using 250 μL collagenase at 950 U/mL in PBS buffer with 1 mM Ca^{2+} (pH 7.0) overnight at 37°C at 1000 rpm. Then 50 μL 2% [w/v] SDS in PBS was added to 25 μL thereof and incubated at 60°C for 10 min. To neutralize the SDS, 25 μL 8% [w/v] IGEPAL in PBS was added followed by addition of 1 μL peptide-*N*-glycosidase F (PNGaseF from *Elizabethkingia meningoseptica* 0.1 U/μL, Bioreagent, Sigma Aldrich) and incubated o/n at 37°C for *N*-glycan liberation. *N*-glycans were labeled with 8-aminopyrene-1,3,6-trisulfonic acid (APTS, Sigma Aldrich) and excess label was removed by hydrophilic-interaction-chromatography (HILIC) using solid phase extraction (SPE) columns with polyacrylamide as stationary phase. Purified APTS-labeled glycans were analyzed by xCGE-LIF. Data processing and migration time normalization to an internal standard were performed with the aid of the glyXtool™ software (glyXera, Magdeburg, Germany). All peaks above a signal to noise ratio of 10 were picked und peak annotation was performed based on normalized electropherograms via migration time matching with the in-house *N*-glycan database (glyXtool™ v. 5.3.0). Peak annotation was confirmed by exoglycosidase digests and repeated analysis by xCGE-LIF. The following enzymes were used: $\alpha(2\text{-}3,6,8)$ sialidase (Sialidase A, Prozyme), $\alpha(1\text{-}3,4,6)$ galactosidase (Prozyme or New England Biolabs (NEB)), $\beta(1\text{-}3)$ galactosidase (NEB), $\alpha(1\text{-}3,4)$ fucosidase (NEB), $\alpha(1\text{-}2,4,6)$ fucosidase (NEB), $\beta(1\text{-}4)$ galactosidase (NEB), and *N*-acetylglucosidaminidase (NEB). Exoglycosidase digestions were carried out as recommended by the respective suppliers; samples were then purified by HILIC-SPE and again analyzed by xCGE-LIF. Glycan signal intensities were calculated for individual peak heights in relation to the sum of all peak heights (signal intensity) and displayed as percent of total peak height (% signal intensity). This analysis reveals how the *N*-glycan pattern behaves between the different samples. However, it does not enable quantitative comparison of glycan levels between the different samples. Thus, we repeated the entire xCGE-LIF analysis upon spiking in 0.083 ng of the glycan neolactotetraose (nLc4) as an internal standard into each sample and displayed the signal intensities as normalized signal intensities in relation to the intensity of the internal standard which was set to one. As the second analysis was performed on a different machine which likely affects the migration times, we did not perform automated glycan assignment but assigned peaks to glycan structures based on the characteristic peak pattern uncovered in the first analysis.

2.4 | Analysis of glycosphingolipid glycosylation

Analysis of glycosphingolipid glycosylation was performed as described previously with minor changes.[28] Glycolipids were extracted from 5 mg (dry weight) of cryogenically grinded porcine pericardia (as described above) in three steps with 1 mL of chloroform/methanol (1:2 (v/v)), chloroform/methanol (2:1 (v/v)) and chloroform/methanol (1:1 (v/v)), respectively, and evaporated to dryness. Glycolipids were dissolved in methanol/water (1:2 (v/v)), desalted on a Chromabond® C_{18} ec polypropylene column (Macherey-Nagel, Düren, Germany) and were eluted and again evaporated to dryness. For glycan release,

glycolipids were incubated with LudgerZyme Ceramide Glycanase (CGase) (Ludger, Oxfordshire, UK) according to the manufacturer's instructions. Released glycans were fluorescently labeled with APTS (Merck). Excess of APTS and reducing agent were subsequently removed by HILIC-SPE. Labeled glycans were eluted, concentrated in a SpeedVac concentrator (Thermo Fisher Scientific) and analyzed by xCGE-LIF. Data were analyzed using the GeneMapper Software v.3.7. We defined a signal having a peak amplitude threshold (as set up in the GeneMapper Software v.3.7) of ≥20 relative fluorescent units (RFU). Annotation of peaks to distinct glycan structures was based on manual migration time matching to our in-house database. For quantitative inter-sample comparison of signal intensities, 0.083 ng of APTS-labelled Glyko® Oligomannose 6 (Man6, Prozyme, Hayward, CA) was spiked into each sample as an internal standard.

3 | RESULTS

3.1 | xCGE-LIF analysis combined with exoglycosidase digests enables reliable *N*-glycan annotation

The xCGE-LIF analysis of differentially treated pericardia (native and decellularized) derived from pigs with different genetic backgrounds (WT, *GGTA1*-KO, *GGTA1/CMAH*-KO) led to the identification of 124 peaks by glyXtool software which were automatically annotated and quantified based on our in-house *N*-glycan database (Figure S1). It should be noted that *N*-glycan levels can be affected by the efficacy of tissue *N*-glycan isolation and the process of glycan labeling. However, these limitations should be similar between the different groups and therefore not interfere with comparative analysis done in this study. To further refine the automatic annotation, we repeated the xCGE-LIF analysis of all samples upon exoglycosidase digestions with α-galactosidase (Figure S2) and sialidase (Figure S3) leading to characteristic peak shifts.

For several *N*-glycans we observed an adjacent peak migrating approximately 8 migration time units (MTU) earlier in our xCGE-LIF analyses. We could provide evidence that these peaks represented labeling artifacts caused by an incomplete labeling reaction (as described in Supplementary Data). However, as we could clearly assign the glycan belonging to these incompletely labeled artifacts, they were included in our further analyses. Altogether, it was possible to specifically annotate 19 peaks representing 11 different biantennary and core-fucosylated *N*-glycans with α-Gal-epitopes and/or terminal sialic acids(s) (e.g., Neu5Ac and Neu5Gc, Figure 1A). These 19 peaks covered the most intense signals in our analyses and together represented more than 47% of the total signal intensity in all 12 samples analyzed.

3.2 | Comparison of relative *N*-glycan intensities between WT, *GGTA1*-KO, and *GGTA1/CMAH*-KO pigs revealed the emergence of neo-glycoepitopes

For the 19 peaks that could unequivocally be assigned to specific *N*-glycans, we compared the changes of relative signal intensities in samples of genetically-modified compared to WT pigs (Figure 1B). As expected, *N*-glycans containing α-Gal-epitopes were—if at all—only detected at background levels in both KO-groups (peaks 58, 59, 60, 61, 91, 93, 95, 96, 102, 105). Accordingly, relative levels of those structures underlying the former α-Gal-epitopes that are terminating with single galactoses were considerably increased (peaks 49, 51, 52, 80, 84). Additionally, *N*-glycans terminating with the sialic acid Neu5Ac (peaks 22, 24, 49, 51) were increased in both, the *GGTA1*-KO and the *GGTA1/CMAH*-KO pericardia, suggesting that the *N*-glycans lacking the α-Gal-epitopes were used by sialyltransferases as acceptors for sialylation. However, these acceptors can be also sialylated with Neu5Gc and accordingly, we detected increased levels of *N*-glycans terminating with Neu5Gc (peaks 25, 26, 52) in the *GGTA1*-KO samples compared to the WT. As expected, these peaks were absent in *GGTA1/CMAH*-KO tissue. However, as Neu5Gc is not available upon deletion of CMAH, levels of *N*-glycans capped with Neu5Ac were increased in *GGTA1/CMAH*-KO pericardia compared to *GGTA1*-KO animals (peaks 22, 24, 49).

3.3 | Determination of normalized *N*-glycan intensities confirmed altered *N*-glycosylation between WT, *GGTA1*-KO, and *GGTA1/CMAH*-KO pigs

The entire xCGE-LIF-based *N*-glycan analysis was repeated upon spike-in of a defined amount of the standard glycan neolactotetraose (nLc4) into each sample. Depending on its specific migration behavior, this standard glycan gives rise to a peak at approximately 466 MTU, a position where it does not interfere with sample peaks. Intensities of all peaks were then scaled to the intensity of the spike-in which was set to 1 for all samples, giving rise to normalized *N*-glycan intensities. Subsequently, we quantitatively determined whole *N*-glycan levels in native and decellularized tissues of WT, *GGTA1*-KO, and *GGTA1/CMAH*-KO animals. Therefore, we summed all normalized intensities of all *N*-glycan signals that were above a defined threshold of two. For WT and *GGTA1*-KO, *N*-glycan levels were considerably higher in decellularized compared to native tissues (Figure 2).

Annotation of peaks in the *N*-glycan analysis with spike-in (for determination of normalized intensities) was adapted from peaks that could clearly be assigned to glycan structures based on the annotation done for the *N*-glycan analysis without spike-in (for determination of relative signal intensities, Figure 1A) (Figure S4A and B). Of note, we observed considerable differences of normalized *N*-glycan
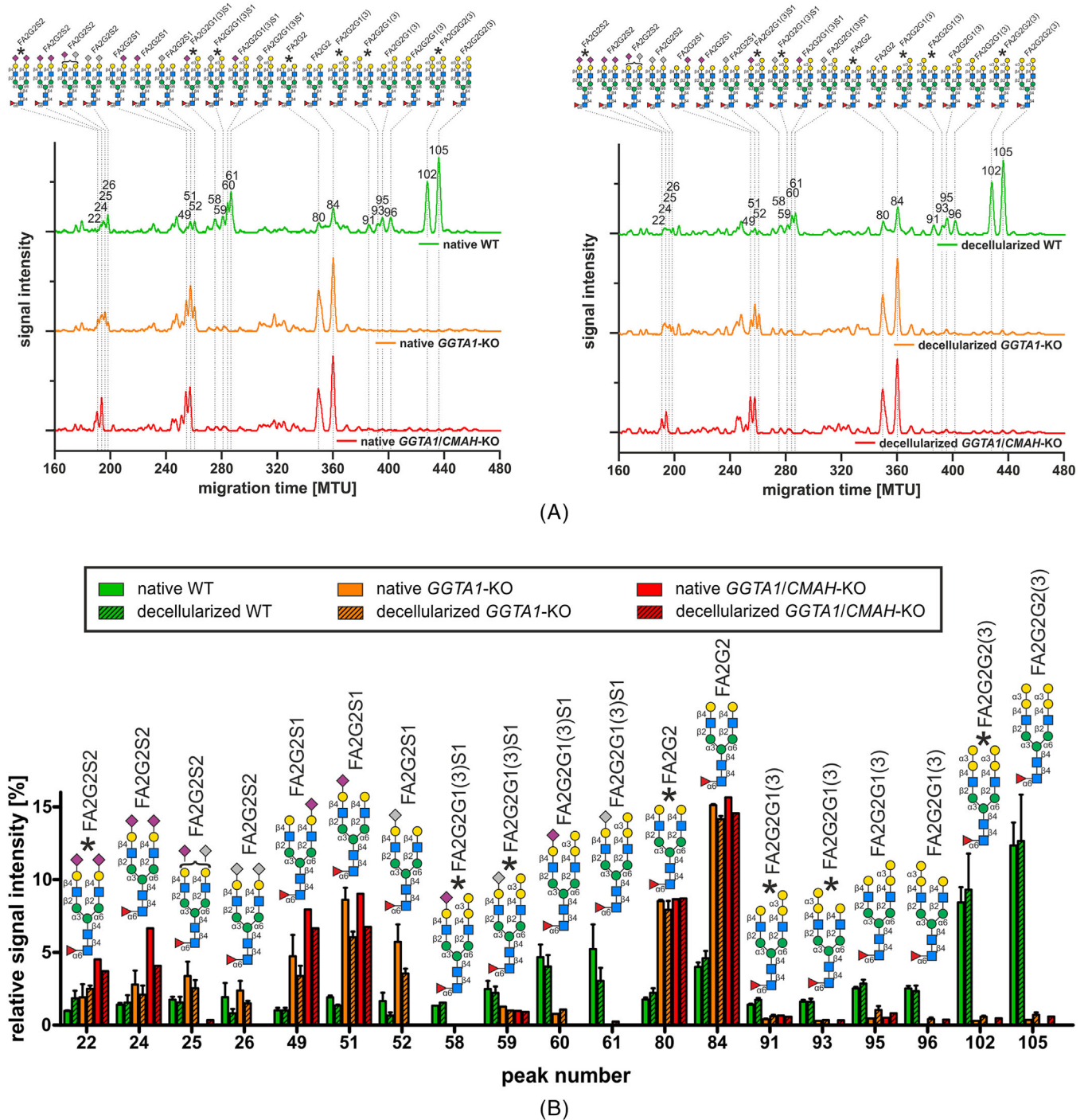
FIGURE 1 Analysis of relative changes of *N*-glycan levels caused by genetic manipulation and/or decellularization of porcine pericardia. (A) Representative xCGE-LIF fingerprints of differentially treated groups for the different genetic backgrounds as indicated. *N*-glycan assignment was based on automated annotation (Figure S1) in combination with exoglycosidase digests (Figures S2–S4). (B) Relative *N*-glycan signal intensities for the differentially treated groups of the different genetic backgrounds as indicated. Bar graphs represent mean values and bars show the standard deviation if applicable. Biological replicates: *n* = 3 for WT native, *n* = 3 for WT decellularized, *n* = 2 for *GGTA1*-KO native, *n* = 2 for *GGTA1*-KO decellularized, *n* = 1 for *GGTA1/CMAH*-KO native, and *n* = 1 for *GGTA1/CMAH*-KO decellularized. Symbol key: blue square: *N*-acetylglucosamine, green circle: mannose, yellow circle: galactose, purple diamond: Neu5Ac, white diamond: Neu5Gc, red triangle: fucose, brace: position of below sugar unclear. The peaks/glycans marked with an asterisk (*) represent incomplete labeling products.
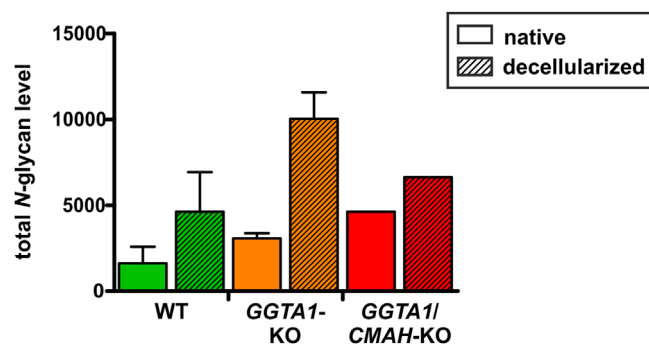
FIGURE 2 Determination of normalized *N*-glycan levels enabling quantitative comparison between different genetically manipulated and/or decellularized groups of porcine pericardia. Accumulated normalized *N*-glycan intensities of all signal peaks above a threshold of 2, calculated individually for the differentially treated groups of the different genetic backgrounds as indicated. Bar graphs represent mean values and bars show standard deviation if applicable. Biological replicates: n = 3 for WT native, n = 3 for WT decellularized, n = 2 for *GGTA1*-KO native, n = 2 for *GGTA1*-KO decellularized, n = 1 for *GGTA1/CMAH*-KO native, and n = 1 for *GGTA1/CMAH*-KO decellularized.

intensities for annotated peaks between the different genetic groups (Figure 4C) which essentially confirmed our findings observed for relative *N*-glycan levels (Figure 1B).

3.4 | Analysis of glycosphingolipid glycosylation shows efficient delipidation by decellularization

We further analyzed glycosylation of GSLs in the different samples by xCGE-LIF upon spike-in of an internal standard enabling the determination of normalized signal intensities. Based on our in-house GSL glycan database most peaks could be assigned to glycan structures (Figure 3). It becomes obvious that normalized glycan intensities are considerably decreased in decellularized compared to native samples, irrespectively of the genetic background (peaks 4, 6, 7, 8, 13, 15, 16, 17, 20, 21). For peaks 9, 11 and 22, decellularization did not affect glycan levels which can be explained by own previous observations that these glycans are a potential contamination originating from impurities of the commercial ceramide glycanase (data not shown). There are no glycan signals that could be detected exclusively in the WT samples but were lacking in samples of both mutants, which should be the case for glycans with α-Gal-epitopes. The GSL-derived glycan GM3 carrying Neu5Ac was detected in all genetic backgrounds. As expected, GM3 carrying Neu5Gc, was detected in WT and *GGTA1*-KO tissues but no signal was observed in the *GGTA1/CMAH*-KO tissues.

4 | DISCUSSION

Porcine pericardium holds great promise to be used as a tissue matrix in xenotransplantation. However, porcine tissue is well known to

be highly immunogenic in the human recipient[29] and in particular porcine pericardium has recently been demonstrated to carry high levels of immunogenic α-Gal and Neu5Gc epitopes attached to *N*- and *O*-glycans.[30] Genetic modification of the donor pig has evolved as an effective strategy to prevent synthesis of immunogenic glycans on porcine organs or tissues thereby facilitating its application in xenotransplantation.[29] Genetically modified pigs lacking the α-Gal and Neu5Gc epitopes have been successfully developed.[31,32] While multi-transgenic and *GGTA1/CMAH/β4GALNT2* triple-glycosyltransferase-KO pig-derived kidney grafts in baboon improve overall xenograft survival, a recent study also demonstrated a rejection reaction based on preformed antibodies potentially directed against neo-antigens of the genetically modified animals.[33] Knocking out glycosyltransferases in the pig to achieve a more human-like glycosylation pattern is expected to cause changes in the porcine glycome that potentially may lead to the emergence of neo-glycoantigens contributing to acute or chronic graft rejection.[23] Thus, here we set out to interrogate the *N*-glycome and the glycosphingolipid-glycome of native and decellularized porcine pericardium comparing WT, *GGTA1* and *GGTA1/CMAH*-KO pigs with the goal to identify potential neo-glycoantigens emerging in these animals. As expected, *N*-glycan analysis revealed that α-Gal or α-Gal/Neu5Gc epitopes were lacking on *N*-glycans derived from porcine pericardium of *GGTA1*- or *GGTA1/CMAH*-KO pigs, respectively. On the other hand, levels of diverse *N*-glycans were considerably affected in both KO groups compared to WT tissue. We observed an increase of sialylated glycans (Neu5Ac and Neu5Gc) in the *GGTA1*-KO group. As the terminal galactose cannot be elongated by a second galactose in the *GGTA1*-KO animals, the available acceptor seems to be used by sialyltransferases for attachment of sialic acids including Neu5Gc, instead. Neu5Gc which is not synthesized in humans has been considered as a major immunogen that might hamper xenotransplantation.[34] Low levels of Neu5Gc can be detected on normal human tissues due to incorporation upon dietary uptake which might induce emergence of anti-Neu5Gc antibodies, but seems to be well tolerated[35] whereas high levels as observed on pig tissues leads to immune reaction. Thus, not only presence but also levels of glycans have to be considered in terms of their immunogenic potential. The present findings demonstrate that KO of *GGTA1* in fact removes the immunogenic α-Gal epitopes but at the expense of increased levels of the immunogenic Neu5Gc epitope. This can be overcome by the combined deletion of *GGTA1* and *CMAH* which prevented synthesis of α-Gal and Neu5Gc epitopes on *N*-glycans. However, *N*-glycan structures terminating either by galactose or by galactose capped with sialic acid were increased in both mutants compared to the WT tissue and these altered distributions of porcine glycan levels cannot be ruled out to be immunogenic in humans.

Similar to *N*-glycans, also GSLs from pig comprise immunogenic glycan determinants.[36] Accordingly, the α-Gal epitope has been detected on porcine GSLs derived from heart and kidney,[37] aortic and pulmonary valve cusps[38] and even pericardia.[39] In contrast to these findings, we did not detect α-Gal epitopes on porcine pericardia in the present study which might be caused by analytical limitations. A further immunogenic sugar present in pigs and associated with
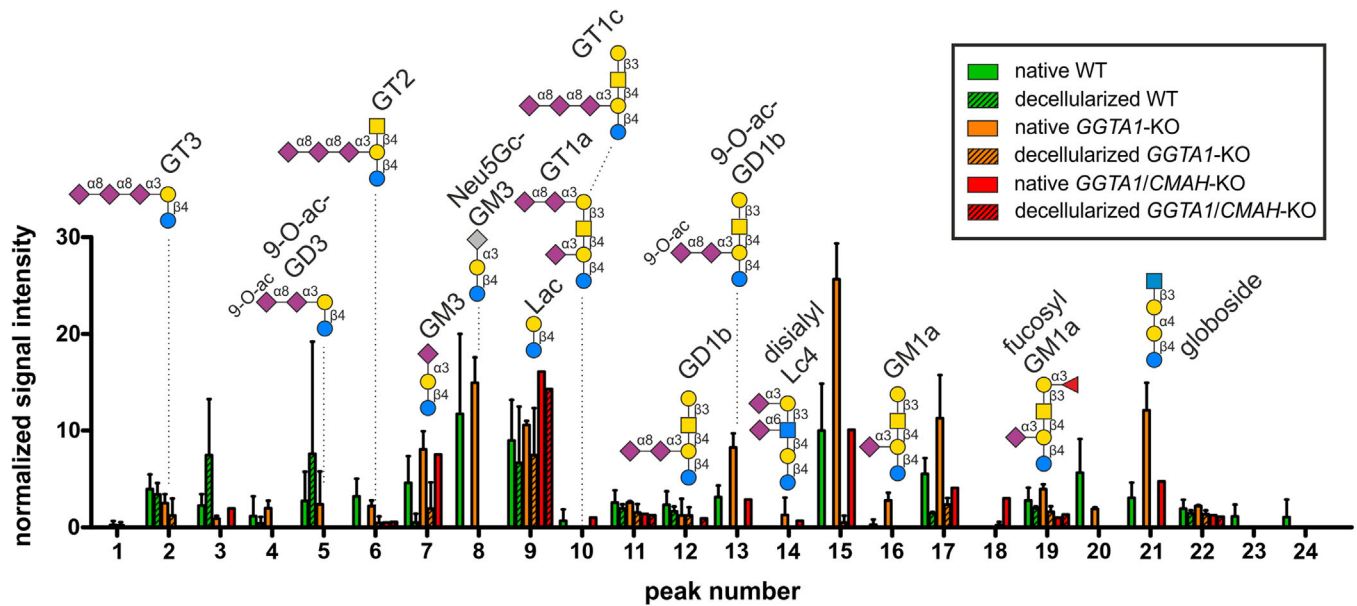
FIGURE 3 Determination of normalized GSL glycosylation of different genetically manipulated and/or decellularized groups of porcine pericardia. Normalized GSL glycan signal intensities for the differentially treated groups of the different genetic backgrounds as indicated. Bar graphs represent mean values and bars show standard deviation if applicable. Biological replicates: $n = 3$ for WT native, $n = 3$ for WT decellularized, $n = 2$ for GGTA1-KO native, $n = 2$ for GGTA1-KO decellularized, $n = 1$ for GGTA1/CMAH-KO native, and $n = 1$ for GGTA1/CMAH-KO decellularized. Symbol key: blue circle: glucose, yellow circle: galactose, yellow square: N-acetylgalactosamine, blue square: N-acetylglucosamine, purple diamond: Neu5Ac, white diamond: Neu5Gc, red triangle: fucose.

xeno-rejection is the sialic acid Neu5Gc.[40,41] Neu5Gc has been detected by immunohistochemistry on porcine BHVs and in native porcine aortic valves and pericardium as well[5,39] whereas it was not found upon analysis of glycosphingolipids on porcine aortic and pulmonary valve cusps.[38] Thus, Neu5Gc has been proposed to be mainly expressed on glycoproteins.[5] However, evidence for the presence of gangliosides capped with Neu5Gc has been provided from pig hearts and kidneys[37] and pericardia.[39] Accordingly, our analytical approach revealed the presence of Neu5Gc-GM3 in pericardium of WT and GGTA1-KO animals while it was absent in GGTA1/CMAH-KO material.

In previous analytical approaches aiming at the identification of porcine xenogeneic glycan-antigens, liquid chromatography coupled to tandem mass spectrometry (LC-MS/MS) was applied for N-glycan analysis[30] while GSL antigens were structurally analyzed by LC-MSMS or proton NMR spectroscopy.[37–39] These methods, which are well suited for (de novo) glycan structure derivation, depend on sophisticated analytical equipment and expertise. The xCGE-LIF approach has also been widely used for N-glycan analysis[42] and we recently showed that it can be employed for glycosphingolipid profiling,[28] which required the establishment of a glycan migration time database. Once such a database has been established, xCGE-LIF allows accurate assignment of glycan structures at medium to high-throughput at low cost.[43] It is limited by size of the database but has the advantage of rapid glycan profiling, for example, for biomedical applications.

Our glycan analyses further revealed that the process of decellularization effectively removed glycosphingolids, including Neu5Gc-GM3 from porcine pericardia. The applied detergents usually disrupt the lipid bilayer of the cells,[44] while the extracellular matrix (ECM) remains

intact.[26,45,46] Accordingly, our previous studies revealed inefficient removal of carbohydrates including α-Gal-epitopes by a detergent-aided decellularization process.[45,47] These findings point towards the ECM as carrier of significant glycosylation. We noted that the applied decellularization did not reduce N-glycan levels as one might expect on the first glimpse. As a potential explanation, we assumed that the decellularization breaks the cells causing removal of cytosolic components which are mostly non-glycosylated while glycosylated ECM proteins are retained. As changes in the N-glycan profile caused by deletion of GGTA1 or GGTA1/CMAH in comparison to WT were similar for native and decellularized tissues, we conclude that the decellularization does not alter the N-glycan profile.

In summary, results of the present study show that interference with the glycosylation machinery by genetic modification of the donor pig does not simply remove the targeted epitopes and thus provides a more humanized glycosylation pattern, but also leads to increased expression or even new appearance of diverse glycan structures, that is, neo-glycans. These glycans might represent neo-antigens and their immunological impact has carefully to be taken into account in xenotransplantation.

AUTHOR CONTRIBUTIONS

CONFLICT OF INTEREST STATEMENT

E.R. is the founder, CEO and CSO of glyXera GmbH. S.C. is employee of glyXera GmbH. glyXera provides high-performance glycoanalytical products and services and holds several patents for xCGE-LIF based glycoanalysis. The other authors declare that they have no conflict of interest.

ORCID

Lucrezia Morticelli https://orcid.org/0000-0003-2890-2156
Samanta Cajic https://orcid.org/0000-0001-5820-0732
Sugat Ratna Tuladhar https://orcid.org/0000-0002-5108-3323
Björn Petersen https://orcid.org/0000-0002-1532-4863
Konrad Fischer https://orcid.org/0000-0002-4926-7334
Erdmann Rapp https://orcid.org/0000-0001-6618-2626
Angelika Schnieke https://orcid.org/0000-0002-5761-9635
Heiner Niemann https://orcid.org/0000-0002-7123-2410
Falk F. R. Buettner https://orcid.org/0000-0002-8468-1223
Andres Hilfiker https://orcid.org/0000-0003-0282-9704

REFERENCES

1. Meier RPH, Muller YD, Balaphas A, et al. Xenotransplantation: back to the future? *Transpl Int*. 2018;31:465–477.
2. Vadori M, Cozzi E. The immunological barriers to xenotransplantation. *Tissue Antigens*. 2015;86:239–253.
3. Rahimtoola SH. Choice of prosthetic heart valve in adults an update. *J Am Coll Cardiol*. 2010;55:2413–2426.
4. Rahmani B, McGregor C, Byrne G, Burriesci G. A durable porcine pericardial surgical bioprosthetic heart valve: a proof of concept. *J Cardiovasc Transl Res*. 2019; 12: 331–337.
5. Reuven EM, Leviatan Ben-Arye S, Marshanski T, et al. Characterization of immunogenic Neu5Gc in bioprosthetic heart valves. *Xenotransplantation*. 2016;23:381–392.
6. Siddiqui RF, Abraham JR, Butany J. Bioprosthetic heart valves: modes of failure. *Histopathology*. 2009;55:135–144.
7. Lee W, Hara H, Cooper DK, Manji RA. Expression of NeuGc on pig heart valves. *Xenotransplantation*. 2015;22:153–154.
8. Naso F, Gandaglia A, Bottio T, et al. First quantification of alpha-Gal epitope in current glutaraldehyde-fixed heart valve bioprostheses. *Xenotransplantation*. 2013;20:252–261.
9. Konakci KZ, Bohle B, Blumer R, et al. Alpha-Gal on bioprostheses: xenograft immune response in cardiac surgery. *Eur J Clin Invest*. 2005;35:17–23.
10. Namiri M, Ashtiani MK, Mashinchian O, et al. Engineering natural heart valves: possibilities and challenges. *J Tissue Eng Regen Med*. 2017;11:1675–1683.
11. Varki A, Sharon N. Historical background and overview. In *Essentials of glycobiology*. Cold Spring Harbor Laboratory Press; 2009.
12. Macher BA, Galili U. The Galalpha1,3Galbeta1,4GlcNAc-R (alpha-Gal) epitope: a carbohydrate of unique evolution and clinical relevance. *Biochim Biophys Acta*. 2008;1780:75–88.
13. Padler-Karavani V and Varki A. Potential impact of the non-human sialic acid N-glycolylneuraminic acid on transplant rejection risk. *Xenotransplantation*. 2011;18:1–5.
14. Salama A, Evanno G, Harb J, Soulillou JP. Potential deleterious role of anti-Neu5Gc antibodies in xenotransplantation. *Xenotransplantation*. 2015;22:85–94.
15. Sandrin MS, McKenzie IF. Gal alpha (1,3)Gal, the major xenoantigen(s) recognised in pigs by human natural antibodies. *Immunol Rev*. 1994;141:169–190.
16. Crapo PM, Gilbert TW, Badylak SF. An overview of tissue and whole organ decellularization processes. *Biomaterials*. 2011;32: 3233–3243.
17. Fischer K, Kraner-Scheiber S, Petersen B, et al. Efficient production of multi-modified pigs for xenotransplantation by 'combineering', gene stacking and gene editing. *Sci Rep*. 2016;6:29081.
18. Lutz AJ, Li P, Estrada JL, et al. Double knockout pigs deficient in N-glycolylneuraminic acid and galactose alpha-1,3-galactose reduce the humoral barrier to xenotransplantation. *Xenotransplantation*. 2013;20:27–35.
19. McGregor CG, Kogelberg H, Vlasin M, Byrne GW. Gal-knockout bioprostheses exhibit less immune stimulation compared to standard biological heart valves. *J Heart Valve Dis*. 2013;22: 383–390.
20. Mohiuddin MM, Singh AK, Corcoran PC, et al. Chimeric 2C10R4 anti-CD40 antibody therapy is critical for long-term survival of GTKO.hCD46.hTBM pig-to-primate cardiac xenograft. *Nat Commun*. 2016;7:11138.
21. Langin M, Mayr T, Reichart B, et al. Consistent success in life-supporting porcine cardiac xenotransplantation. *Nature*. 2018; 564: 430–433.
22. Miyagawa S, Yamamoto A, Matsunami K, et al. Complement regulation in the GalT KO era. *Xenotransplantation*. 2010;17:11–25.
23. Burlak C, Bern M, Brito AE, et al. N-linked glycan profiling of GGTA1/CMAH knockout pigs identifies new potential carbohydrate xenoantigens. *Xenotransplantation*. 2013;20:277–291.
24. Yeh P, Ezzelarab M, Bovin N, et al. Investigation of potential carbohydrate antigen targets for human and baboon antibodies. *Xenotransplantation*. 2010;17:197–206.
25. Petersen B, Frenzel A, Lucas-Hahn A, et al. Efficient production of biallelic GGTA1 knockout pigs by cytoplasmic microinjection of CRISPR/Cas9 into zygotes. *Xenotransplantation*. 2016;23:338–346.
26. Theodoridis K, Muller J, Ramm R, et al. Effects of combined cryopreservation and decellularization on the biomechanical, structural and biochemical properties of porcine pulmonary heart valves. *Acta Biomater*. 2016;43:71–77.
27. Hennig R, Rapp E, Kottler R, Cajic S, Borowiak M, Reichl U. N-glycosylation fingerprinting of viral glycoproteins by xCGE-LIF. *Methods Mol Biol*. 2015;1331:123–143.
28. Rossdam C, Konze SA, Oberbeck A, et al. Approach for profiling of glycosphingolipid glycosylation by multiplexed capillary gel electrophoresis coupled to laser-induced fluorescence detection to identify cell-surface markers of human pluripotent stem cells and derived cardiomyocytes. *Anal Chem*. 2019;91:6413–6418.

29. Lu T, Yang B, Wang R, Qin C. Xenotransplantation: current status in preclinical research. *Front Immunol*. 2019;10:3060.

30. Jin C, Cherian RM, Liu J, et al. Identification by mass spectrometry and immunoblotting of xenogeneic antigens in the *N*- and *O*-glycomes of porcine, bovine and equine heart tissues. *Glycoconj J*. 2020;37:485–498.

31. Fischer K, Rieblinger B, Hein R, et al. Viable pigs after simultaneous inactivation of porcine MHC class I and three xenoreactive antigen genes GGTA1, CMAH and B4GALNT2. *Xenotransplantation*. 2020;27:e12560.

32. Hein R, Sake HJ, Pokoyski C, et al. Triple (GGTA1, CMAH, B2M) modified pigs expressing an SLA class I(low) phenotype-effects on immune status and susceptibility to human immune responses. *Am J Transplant*. 2020;20:988–998.

33. Ariyoshi Y, Takeuchi K, Pomposelli T, et al. Antibody reactivity with new antigens revealed in multi-transgenic triple knockout pigs may cause early loss of pig kidneys in baboons. *Xenotransplantation*. 2021;28:e12642.

34. Tector AJ, Mosser M, Tector M, Bach JM. The possible role of anti-Neu5Gc as an obstacle in xenotransplantation. *Front Immunol*. 2020;11:622.

35. Tangvoranuntakul P, Gagneux P, Diaz S, et al. Human uptake and incorporation of an immunogenic nonhuman dietary sialic acid. *Proc Natl Acad Sci USA*. 2003;100:12045–12050.

36. Jang KS, Kim YG, Adhya M, Park HM, Kim BG. The sweets standing at the borderline between allo- and xenotransplantation. *Xenotransplantation*. 2013;20:199–208.

37. Diswall M, Angstrom J, Karlsson H, et al. Structural characterization of alpha1,3-galactosyltransferase knockout pig heart and kidney glycolipids and their reactivity with human and baboon antibodies. *Xenotransplantation*. 2010;17:48–60.

38. Barone A, Benktander J, Teneberg S, Breimer ME. Characterization of acid and non-acid glycosphingolipids of porcine heart valve cusps as potential immune targets in biological heart valve grafts. *Xenotransplantation*. 2014;21:510–522.

39. Barone A, Benktander J, Whiddon C, et al. Glycosphingolipids of porcine, bovine, and equine pericardia as potential immune targets in bioprosthetic heart valve grafts. *Xenotransplantation*. 2018;25:e12406.

40. Breimer ME. Gal/non-Gal antigens in pig tissues and human non-Gal antibodies in the GalT-KO era. *Xenotransplantation*. 2011;18:215–228.

41. Breimer ME, Holgersson J. The structural complexity and animal tissue distribution of *N*-glycolylneuraminic acid (Neu5Gc)-terminated glycans. Implications for their immunogenicity in clinical xenografting. *Front Mol Biosci*. 2019;6:57.

42. Lu G, Crihfield CL, Gattu S, Veltri LM, Holland LA. Capillary electrophoresis separations of glycans. *Chem Rev*. 2018;118:7867–7885.

43. Huffman JE, Pucic-Bakovic M, Klaric L, et al. Comparative performance of four methods for high-throughput glycosylation analysis of immunoglobulin G in genetic and epidemiological research. *Mol Cell Proteomics*. 2014;13:1598–1610.

44. Naso F, Gandaglia A. Different approaches to heart valve decellularization: a comprehensive overview of the past 30 years. *Xenotransplantation*. 2018;25:e12354.

45. Findeisen K, Morticelli L, Goecke T, et al. Toward acellular xenogeneic heart valve prostheses: histological and biomechanical characterization of decellularized and enzymatically deglycosylated porcine pulmonary heart valve matrices. *Xenotransplantation*. 2020;27:e12617.

46. Ramm R, Goecke T, Theodoridis K, et al. Decellularization combined with enzymatic removal of N-linked glycans and residual DNA reduces inflammatory response and improves performance of porcine xenogeneic pulmonary heart valves in an ovine in vivo model. *Xenotransplantation*. 2020;27:e12571.

47. Ramm R, Niemann H, Petersen B, Haverich A, Hilfiker A. Decellularized *GGTA1*-KO pig heart valves do not bind preformed human xenoantibodies. *Basic Res Cardiol*. 2016;111:39.

SUPPORTING INFORMATION

Additional supporting information can be found online in the Supporting Information section at the end of this article.